Chemical forms of molybdenum ion in nitric acid solution studied using liquid-phase X-ray absorption fine structure, Ultraviolet-Visible absorption spectroscopy and first-principles calculations

Shinta Watanabe[a,*], Toshikazu Sato[a], Masato Nakaya[a], Tomoko Yoshida[b], Jun Onoe[a,*]

[a]Department of Energy Science and Engineering, Nagoya University, Furo-cho, Chikusa-ku, Nagoya, Aichi 464-8603, Japan

[b]Advanced Research Institute for Natural Science and Technology, Osaka City University 3-3-138 Sugimoto, Osaka-shi, Osaka, 558-8585, Japan

Corresponding Authors

* E-mail address: s-watanabe@energy.nagoya-u.ac.ne.jp (S. Watanabe) and

j-onoe@energy.nagoya-u.ac.ne.jp (J. Onoe)

Keywords: Molybdenum, XAFS, First-principles calculations, High-level radioactive nuclear liquid wastes, Vitrification processes

ABSTRACT

We have investigated chemical forms of molybdenum ion in nitric acid solution, using liquid-phase X-ray absorption fine structure, ultraviolet-visible absorption spectroscopy and first-principles calculations, from a viewpoint of disposal of high-level radioactive nuclear liquid wastes. The experimental and theoretical results indicated that Mo is a hexavalent ion and forms a hexa-coordination binuclear-structured complex in the 2 M nitic acid solution. The predominant chemical species of Mo complexes in the 2 M nitric acid solution (which is used for HLLW) are assigned to be $[Mo_2O_5(H_2O)_6]^{2+}$ and $[Mo_2O_4(OH)(H_2O)_6]^{3+}$. These species may play a crucial role of forming so-called yellow-phase in vitrified objects.

1. Introduction

High-level radioactive liquid wastes (HLLW) in 2 M nitric acid solution, which are generated in the reprocessing of spent nuclear fuels, have been vitrified by using a Joule-heating based melter in Japan [1, 2]. Molybdenum (Mo), which is one of the major fission products of the spent nuclear fuels, forms the compounds isolated in the vitrified object. These Mo compounds, so called "yellow phase", cause serious problems in the vitrification processes of HLLW: the degradation of vitrified objects due to heterogenization [3]. To solve these issues, we have proposed a process for efficient removal of Mo (as well as Platinum-group elements (Ruthenium, Rhodium, Palladium) from HLLW prior to introducing into the glass melter, using metal hexacyanoferrates (HCF) used as a sorbent [4-6]. In this process, chemical forms of Mo ion in pure nitric acid solution are one of the important information for the clarification of sorption mechanisms of Mo into HCF. In addition, this information will play a key role of designing a high-performance sorbent for removal of Mo from HLLW.

Chemical forms of Mo ion in solution have been extensively studied in association with polyoxomolybdates, which have drawn attention not only in the field of inorganic chemistry [7-9] but also in the industrial field [10,11]. In the previous studies, many chemical species of Mo complexes in solution have been found. Especially, the predominant species such as $[MoO_4]^{2-}$, $[HMoO_4]^{-}$, $[Mo_7O_{24}]^{6-}$, $[HMo_7O_{24}]^{5-}$, $[H_2Mo_7O_{24}]^{4-}$, and $[Mo_8O_{26}]^{4-}$ strongly depend on the ionic strength, Mo concentration, and pH [7, 12-21]. However, there have been a few reports on Mo complexes in strong acid solutions so far [7, 19]. In particular, a study for chemical forms of Mo ion in pure nitric acid solution has been limited.

From the perspective of vitrification processing, the structural and thermodynamic properties of the yellow phase in vitrified objects have been studied by X-ray absorption fine structure (XAFS) [22-25] and isobaric heat capacity [26, 27] measurements. Since these works mainly investigated the characteristics of Mo in the glass (solid phase), there has been little information on chemical forms of Mo ion in nitric acid solution. Accordingly, it is important to clarify the chemical forms for developing vitrification processes.

The aim of the present study is to clarify chemical forms of Mo ion in pure nitric acid solution, using liquid-phase XAFS and UV-Vis spectroscopy in combination with first-principles calculations.

2. Experimental methods.

Mo complexes in nitric acid solution and pure water were prepared by dissolving $Na_2MoO_4 \cdot 2H_2O$ (Wako, 99.0 %). UV-Vis absorption spectra of Mo complexes ([Mo] = 2×10^{-2} M, [HNO3] = 0, 1×10^{-2}, 1×10^{-1}, 1 and 2 M) were recorded using JASCO UV-630 spectrometer. Since the absorption of nitric acid itself in the UV region is very intense, these measurements were performed using a cell with an optical path-length of 0.01 mm. The absorption signal form the nitric acid was subtracted from the nitric acid solution in the same concentration as the background. Mo *K*-edge XAFS spectra of the Mo complexes ([Mo] = 1×10^{-1} M) both in 2 M nitric acid solution and in aqueous solution and of the reference materials such as MoO_3 and $Na_2MoO_4 \cdot 2H_2O$ were measured in transmittance mode, using a synchrotron radiation (SR) light source at AR-NW10A beam line of Photon Factory at the Institute of Materials Structure Science.

3. Theoretical methods.

Geometry optimizations of Mo complexes were performed using the Gaussian09 [28] based on DFT [29, 30]. The def2-TZVP basis set [31] was used for all atoms. In the case of Mo, inner-shell electrons were replaced with the effective core potential [32]. The exchange-correlation potential was considered using the Coulomb-attenuating method (CAM-B3LYP) [33]. The polarizable continuum model was employed to consider the solvent effects of water by using the integral equation formalism variant (IEFPCM) [34]. The free-energy change (ΔG) of the condensation reactions was estimated by frequency calculations of the optimized structures at 298.15 K and 1 atm. Theoretical UV-Vis absorption spectra originating from the ligand to metal charge transfer (LMCT) for the optimized structure of Mo complexes were obtained by TDDFT method [35]. The basis set and exchange-correlation functional used were the same as for the optimization calculations. The solvent effects of water were also considered in all TDDFT calculations.

The *K*-edge X-ray absorption near edge structure (XANES) spectra and the corresponding multiplet energy levels were calculated using the first-principles relativistic configuration interaction (CI) method [36, 37]. In the present CI calculations, MoO_4^{2-} and MoO_6^{4-} model clusters were employed as four and six coordinated Mo complex models, respectively. Four-component relativistic molecular orbital (MO) spinors were obtained using relativistic DFT calculations in which the four-component Dirac equation was solved directly [38]. The relativistic formalism of the VWN exchange-correlation potential [39, 40] was considered. After the one-electron relativistic DFT calculations, many-electron calculations were performed using the relativistic MO spinors. The MOs mainly composed of Mo-1s, 4d, 5s and 5p orbitals were explicitly treated as the active space of the CI calculations. Therefore, the active space of the CI

calculations is composed of 2 electrons in 20 MO spinors, which correspond to the 190 Slater determinants as the basis for CI calculations. The many-electron Dirac-Coulomb-Breit Hamiltonian was employed throughout the present calculations. Details of the computational procedures for the present CI method have been described in Ref. 37.

4. Results and discussion

The thermodynamic stability of individual Mo complexes has been reported comprehensively by Duarte et al [41], and the synthesis path of $[Mo_8O_{26}]^{4-}$ full name (POMs) was well explained by DFT calculations. However, when the actual HLLW is considered, it is necessary to calculate the chemical species of Mo complexes under strongly acidic conditions. Therefore, we first examined the thermodynamic stability of the four species, $MoO_3(H_2O)_3$, $[MoO_2(OH)(H_2O)_3]^+$, $[Mo_2O_5(H_2O)_6]^{2+}$, $[Mo_2O_4(OH)(H_2O)_6]^{3+}$, under strongly acidic conditions, which were reported by Cruywagen [7]. As an initial Mo complex of the condensation reaction, we adopted $[MoO_4]^{2-}$ complex, which is easily considered to be formed by dissolving Na_2MoO_4 solid in the solution. Figure 1 schematically illustrates the free energy diagram for individual condensation reactions of the Mo complexes. The corresponding reaction formulas and the ΔG values are listed in Table 1.

As shown in Fig. 1, the product of the mononuclear complexes in the condensation reactions becomes stabilized as the reaction progresses [reactions (1) and (2)], whereas that of the binuclear complex does slightly destabilized as the reaction progresses [reactions (3) and (4)]. Reaction (3), polynuclearization, strongly depends on the concentration of Mo ion, whereas reaction (4) strongly depends on the pH of nitric acid solution [7]. Since it is difficult to

reproduce these exact conditions using present theoretical calculations, it seems to influence the ΔG value. However, the ΔG for reaction (3) and (4) was obtained to be small, 0.04 eV (3.77 kJ/mol) and 0.17 eV (16.06 kJ/mol), respectively. Since the actual HLLW is treated under strong acid condition at ca. 80 °C, those reactions are expected to proceed easily under the actual conditions. Hence, it can be concluded that the binuclear complexes, $[Mo_2O_5(H_2O)_6]^{2+}$ and $[Mo_2O_4(OH)(H_2O)_6]^{3+}$, are thermodynamically stable in the actual HLLW.

Figure 2 shows the Mo *K*-edge XANES spectra for Mo complexes in 2 M nitric acid solution (red) and in aqueous solution (blue) along with those of the reference materials such as $Mo(VI)O_3$ (green) and $Na_2Mo(IV)O_4{\cdot}2H_2O$ (pink). Since the main absorption edges corresponding to the 1s – 5p transitions (see arrow 1 in Fig. 2) for the XANES spectra of Mo complexes in both aqueous and nitric acid solutions were observed at almost the same energy as for $Mo(VI)O_3$, Mo is a hexavalent ion in both the solutions. On the other hand, the pre-edge peaks (see arrow 2 in Fig. 2) of Mo complexes in both aqueous and nitric acid solutions were significantly different from each other, and the spectral shapes of Mo complexes in the aqueous and nitric acid solutions were in good agreement with those of $Na_2Mo(IV)O_4{\cdot}2H_2O$ and $Mo(VI)O_3$, respectively.

Why did the pre-edge peaks show the different behavior when compared to the main edge ones? This is caused by the difference in their coordination environments. We next analyzed the experimental XANES spectra of Fig. 2 by the first-principles CI calculations to reveal the reason behind the difference. Figure 3 shows the theoretical Mo K-edge XANES spectra (top) and multiplet energy levels with the corresponding transition components (bottom) for four- and six-coordinated Mo complexes shown in inset. The four- and six-coordinated Mo complex models were constructed from the crystalline structure of $Na_2MoO_4{\cdot}2H_2O$ and MoO_3, respectively. Each

intense main-edge peak appearing around 20000 eV was found to originate mainly from the 1s-5p transitions of Mo atom, and these have almost the same spectral shape as for both Mo complexes. On the other hand, there is some significant difference in the spectral shape of the pre-edge peak between the four- and six-coordinated Mo complex models. The pre-edge peaks were both dominantly attributed to the 1s-4d transitions of Mo atom (though the 1s-5p transitions are slightly mixed). In these transitions, the electric dipole transitions are inherently forbidden, but those occur due to the 4d-5p hybridization. The magnitude of 4d-5p hybridization for the four-coordinated Mo complex is greater than that for the six-coordinated one, because the 4d and 5p orbitals have the same symmetry (t_2) for the former complex. In addition to the electric quadrupole transitions to the Mo-4d orbitals, since the components of the electric dipole 1s-5p transitions contribute more remarkably to the pre-edge peak for the four-coordinated complex, the intensity of the pre-edge peak becomes strengthened compared to that for the six-coordinated complex. Consequently, these factors cause the difference in the spectral shape of the pre-edge peaks of Mo complexes in between aqueous and nitric acid solutions.

We next examined the fine structural information on Mo complexes in aqueous and nitric acid solutions, using extended X-ray absorption fine structure (EXAFS) with consideration of the phase correction. Figure 4 shows (a) the radial distribution functions (RDFs) of the Mo complex in aqueous (blue) and 2 M nitric acid (red) solutions, $Na_2MoO_4 \cdot 2H_2O$ (pink) and MoO_3 (green) which were obtained experimentally, and (b) the RDFs obtained using the FEFF [42, 43] calculations of the $[Mo_2O_5(H_2O)_6]^{2+}$ and $[Mo_2O_4(OH)(H_2O)_6]^{3+}$ complex models. As shown in Fig. 4 (a), the overall features of the RDFs for the Mo complex in aqueous (blue) and 2 M nitric acid (red) solutions are basically in good agreement with those for the $Na_2Mo(IV)O_4 \cdot 2H_2O$ (pink) and $Mo(VI)O_3$ (green), respectively. When the RDF of Mo complex is compared between

in 2 M nitric acid solution (red) and in aqueous solution (blue), the scattering effects with the first nearest-neighboring Mo atoms were observed in the range of 3.2–3.6 Å in the former solution, whereas they were not observed in the latter one. On the other hand, the scattering effects from the second nearest-neighboring Mo atoms were observed at ca. 5.2 Å for MoO_3 (green), whereas they were not observed for Mo complex in 2 M nitric acid solution (red). This suggests that Mo atom in 2 M nitric acid solution forms binuclear complexes and they separately exist in the solution. In the case of $Na_2MoO_4 \cdot 2H_2O$, since each MoO_4 is a relatively discrete unit in the solid phase (the distance between adjacent Mo atoms is 4.42 Å), the RDFs between $[MoO_4]^{2-}$ units in aqueous solution (blue) were in a reasonable agreement with those for $Na_2MoO_4 \cdot 2H_2O$ solid phase (pink).

To understand the difference in the results of RDFs between aqueous and 2M nitric acid solutions, we calculated the FEFF of RDFs for the $[Mo_2O_5(H_2O)_6]^{2+}$ (top) and two $[Mo_2O_4(OH)(H_2O)_6]^{3+}$ complex models (I: middle, II: bottom) [Fig. 4 (b): each line represents the oxygen and molybdenum components shown by the same corresponding color], and schematically illustrated each model [Fig. 4(c)] that was optimized using DFT calculations. In case of $[Mo_2O_5(H_2O)_6]^{2+}$, two Mo atoms are in an equivalent environment with four types of first-nearest neighboring oxygen atoms: one bridged between the two Mo atoms (O-Mo, red), two terminal oxygens (O, black), and two types of oxygens for the H_2O molecule (O-$H_2$1, 2, green and blue). On the other hand, in case of $[Mo_2O_4(OH)(H_2O)_6]^{3+}$ (model I and II), two Mo atoms are in different environments. Model I has oxygen bridged between Mo atoms (O-Mo, red), two terminal oxygens (O, black), and three types of oxygens for the H_2O molecule (O-$H_2$1, 2, 3, green, blue and light blue), whereas model II has oxygen bridged between Mo atoms (O-Mo, red), one terminal oxygen (O, black), two types of oxygens for the H_2O molecule (O-$H_2$1, 2, blue

and light blue), and one oxygen for OH (O-H, green). In addition to these oxygen species, the scattering effects by the first-nearest neighboring Mo atoms were also taken into account (pink) in all FEFF calculations. As shown in Fig. 4 (b), $[Mo_2O_5(H_2O)_6]^{2+}$ and $[Mo_2O_4(OH)(H_2O)_6]^{3+}$ complex models qualitatively reproduced the experimental RDF for the Mo complex in 2 M nitric acid solution. The peak appearing in the range 1-2 Å [red in Fig. 4 (a)] is split and broad, which are due to the difference in the first-nearest neighboring oxygen species, whereas the peak observed in the range 3.2–3.6 Å was attributed to the scattering effects in between Mo atoms. These results indicate that the Mo atoms in 2 M nitric acid solution form the hexa-coordination binuclear complex.

We next examined UV-Vis absorption spectra of Mo complexes in aqueous and nitric acid [0.01, 0.1, 1 and 2 M] solution, as shown in Fig. 5. It is noted that saturation of the absorption spectra at wavelengths shorter than 250 nm for the Mo complex in 1 and 2 M nitric acid solution is due to the strong absorption of nitric acid in the region. The absorption edge of the UV-Vis spectra became shifted gradually to a longer wavelength with increasing the nitric acid concentration from 0 to 2 M. This suggests that the predominant chemical species of the Mo complex in solution were changed. Figure 6 shows the theoretical absorption spectra of $[MoO_4]^{2-}$, $[MoO_2(OH)(H_2O)_3]^{+}$, $[Mo_2O_5(H_2O)_6]^{2+}$, $[Mo_2O_4(OH)(H_2O)_6]^{3+}$ models by using Time-dependent DFT (TDDFT) method. The absorption edge of the Mo complexes was observed at a longer wavelength as the condensation reaction progresses, which qualitatively explained the dependence of the nitric acid concentration on the experimental spectra. As the concentration of nitric acid increased, the chemical form of the Mo complex was changed from a tetra-coordination structure to a hexa-coordination one, and finally formed a binuclear complex that depends on the Mo concentration. This is consistent with the previous results [7].

The present study found that the main component of Mo complex in nitric acid solution strongly depends on the pH and Mo concentration, and the binuclear complex is formed in the same environment as in HLLW. When we consider the proposed processes where Mo is effectively removed from HLLW prior to being introduced into the glass melter by using metal HCF used as a sorbent, the present findings leading to control the solution environment of the Mo complex would be useful for an efficient removal of Mo from HLLW.

4. Conclusions

We have investigated the chemical form of Mo atom in nitric acid solution, using XAFS/UV-Vis spectroscopy and first-principles calculation methods. DFT calculations predicted that the binuclear complexes, such as $[Mo_2O_5(H_2O)_6]^{2+}$ and $[Mo_2O_4(OH)(H_2O)_6]^{3+}$, are thermodynamically stable in the HLLW environment (2 M nitric acid solution). Comparison between XAFS/UV-Vis spectra and the first-principles relativistic CI and TDDFT calculated results indicated that Mo atom in nitric acid solution is a hexavalent ion and forms a hexa-coordinated binuclear structure, whereas a tetra-coordinated mononuclear structure in aqueous solution. Judging from the experimental and theoretical results, it is reasonably concluded that the predominant chemical species of Mo complex are $[Mo_2O_5(H_2O)_6]^{2+}$ and $[Mo_2O_4(OH)(H_2O)_6]^{3+}$ in 2M nitric acid solution. These findings are important to develop the vitrification processes for disposal of HLLW.

ACKNOWLEDGEMENTS

The present work was financially supported by “The R&D program for advanced nuclear power systems” organized by MEXT (Ministry of Education, Culture, Sports, Science and Technology).

REFERENCES

[1] M. Yoshioka, S. Torata, H. Igarashi, T. Takahashi, and M. Horie, Waste Management 12 (1992) 7.

[2] Kanehira, Norio; Yoshioka, Masahiro; Muramoto, Hitoshi; Oba, Takaaki; Takahashi, Yuji, Melter operation results in chemical test at Rokkasho reprocessing plant. Proc. GLOBAL 2005, Tsukuba, Japan, 9-13 October; 2005.

[3] Y. Kawamoto, K. Clemens, and M. Tomozawa, J. Am. Ceram. Soc. 64 (1981) 289.

[4] K. Takeshita, Y. Inaba, H. Takahashi, J. Onoe, and H. Narita, Development of Separation Process of PGMs and Mo from High-level Liquid Waste for the Stable Operation of Vitrification Process. Proceedings of Global 2015, Sept. 20-24; 2015.

[5] T. Onishi, K. Sekioka, M. Suto, K. Tanaka, S. Koyama, Y. Inaba, H. Takahashi, M. Harigai, K. Takeshita, Energy Procedia 131 (2017) 151.

[6] S. Watanabe, T. Sato, T. Yoshida, M. Nakaya, M. Yoshino, T. Nagasaki, Y. Inaba, K. Takeshita, and J. Onoe, AIP advances 8, (2018) 045221.

[7] J. J. Cruywagen, Adv. Inorg. Chem. 49 (2000) 127.

[8] M. Cindrić, Z. Veksli, and B. Kamenar, Croat. Chem. Acta 82 (2009) 345.

[9] De-L. Long, R. Tsunashima, and L. Cronin, Angew. Chem. Int. Ed. 49 (2010) 1736.

[10] J. T. Rhule, C. L. Hill, and D. A. Judd, Chem. Rev. 98 (1998) 327.

[11] Sa-Sa Wang, and Guo-Yu Yang, Chem. Rev. 115 (2015) 4893.

[12] A. Yagasaki, and Y. Sasaki, Bull. Chem. Soc. Jpn. 60 (1987) 763.

[13] A. Yagasaki I. Andersson, and L. Pettersson, Inorg. Chem. 26 (1987) 3926.

[14] J. J. Cruywagen, A. G. Draaijer, J. B. B. Heyns, and E. A. Rohwer, Inorg. Chim. Acta 331 (2002) 322.

[15] I. Lj. Validzic, G. van Hooijdonk, S. Oosterhout, and W. K. Kegel, Langmuir 20 (2004) 3435.

[16] P. Tkac, and A. Paulenova, Sep. Sci. Technol. 43 (2008) 2641.

[17] O. F. Oyerinde, C. L. Weeks, A. D. Anbar, and T. G. Spiro, Inorg. Chim. Acta 361 (2008) 1000.

[18] L. Zeng, and C. Y. Cheng, Hydrometallurgy 98 (2009) 10.

[19] M. Lee, S. Sohn, and M. Lee, Bull. Korean Chem. Soc. 32 (2011) 3687.

[20] A. Davantès, and G. Lefèvre, J. Phys. Chem. A 117 (2013) 12922.

[21] J. Torres, L. Gonzatto, G. Peinado, C. Kremer, and E. Kremer, J Solution Chem. 43 (2014) 1687.

[22] G. Calas, M. Le Grand, L. Galoisy, and D. Ghaleb, J. Nucl. Mater. 322 (2003) 15.

[23] R. J. Short, R. J. Hand, N. C. Hyatt, and G. Möus, J. Nucl. Mater. 340 (2005) 179.

[24] O. Pinet, J. L. Dussossoy, C. David, and C. Fillet, J. Nucl. Mater. 377 (2008) 307.

[25] D. A. McKeown, H. Gan, and I. L. Pegg, J. Nucl. Mater. 488 (2017) 143.

[26] M. Morishita, Y. Kinoshita, H. Houshiyama, A. Nozaki, and H. Yamamoto, J. Chem. Thermodyn. 114 (2017) 30.

[27] M. Morishita, Y. Kinoshita, H. Tanaka, A. Nozaki, and H. Yamamoto, Monatsh. Chem. 149 (2018) 341.

[28] M. J. Frisch, G. W. Trucks, H. B. Schlegel, G. E. Scuseria, M. A. Robb, J. R. Cheeseman, G. Scalmani, V. Barone, G. A. Petersson, H. Nakatsuji, X. Li, M. Caricato, A. Marenich, J. Bloino, B. G. Janesko, R. Gomperts, B. Mennucci, H. P. Hratchian, J. V. Ortiz, A. F. Izmaylov, J. L. Sonnenberg, D. Williams-Young, F. Ding, F. Lipparini, F. Egidi, J. Goings, B. Peng, A. Petrone, T. Henderson, D. Ranasinghe, V. G. Zakrzewski, J. Gao, N. Rega, G. Zheng, W. Liang, M. Hada, M. Ehara, K. Toyota, R. Fukuda, J. Hasegawa, M. Ishida, T. Nakajima, Y. Honda, O. Kitao, H. Nakai, T. Vreven, K. Throssell, J. A. Montgomery, Jr., J. E. Peralta, F. Ogliaro, M. Bearpark, J. J. Heyd, E. Brothers, K. N. Kudin, V. N. Staroverov, T. Keith, R. Kobayashi, J. Normand, K. Raghavachari, A. Rendell, J. C. Burant, S. S. Iyengar, J. Tomasi, M. Cossi, J. M. Millam, M. Klene, C. Adamo, R. Cammi, J. W. Ochterski, R. L. Martin, K. Morokuma, O. Farkas, J. B. Foresman, and D. J. Fox, Gaussian 09, Revision D.01, Gaussian, Inc., Wallingford CT, 2013.

[29] P. Hohenberg, W. Kohn, Phys. Rev. 136 (1964) B864.

[30] W. Kohn, L. J. Sham, Phys. Rev. 140 (1965) A1133.

[31] F. Weigend, and R. Ahlrichs, Phys. Chem. Chem. Phys. 7 (2005) 3297.

[32] D. Andrae, U. Häußermann, M. Dolg, H. Stoll, and H. Preuß, Theor. Chem. Acta. 77 (1990) 123.

[33] T. Yanai, D. P. Tew, and N. C. Handy, Chem. Phys. Lett. 393 (2004) 51.

[34] J. Tomasi, B. Mennucci, and R. Cammi, Chem. Rev. 105 (2005) 2999.

[35] E. Runge, and E. K. U. Gross, Phys. Rev. Lett. 52 (1984) 997.

[36] K. Ogasawara, T. Iwata, Y. Koyama, T. Ishii, I. Tanaka, and H. Adachi, Phys. Rev. B 64 (2001) 115413.

[37] S. Watanabe, K. Ogasawara, M. Yoshino, and T. Nagasaki, Phys. Rev. B 81 (2010) 125128.

[38] A. Rosén, D. E. Ellis, H. Adachi, F. W. Averill, J. Chem. Phys. 65 (1976) 3629.

[39] S. H. Vosko, L. Wilk, M. Nusair, Can. J. Phys. 58 (1980) 1200.

[40] A. H. MacDonald, S. H. Vosko, J. Phys. C: Solid State Phys. 12 (1979) 2977.

[41] F. Steffler, G. F. de Lima, and H. A. Duarte, Chem. Phys. Lett. 669 (2017) 104.

[42] J. J. Rehr, S. I. Zabinsky, and R. C. Albers, Phys. Rev. Lett. 69, (1992) 3397.

[43] J. J. Rehr, J. Mustre de Leon, S. I. Zabinsky, and R. C. Albers, J. Am. Chem. Soc. 113 (1991) 5135.

Table 1. The free-energy change (ΔG) of the condensation reactions for Mo complexes.

condensation reaction	ΔG (eV)
(1) $MoO_4^{2-} + 2H_3O^+ \rightarrow MoO_3(H_2O)_3$	-2.99
(2) $MoO_3(H_2O)_3 + H_3O^+ \rightarrow MoO_2(OH)(H_2O)_3^+ + H_2O$	-1.21
(3) $2[MoO_2(OH)(H_2O)_3^+] \rightarrow Mo_2O_5(H_2O)_6^{2+} + H_2O$	0.04
(4) $Mo_2O_5(H_2O)_6^{2+} + H_3O^+ \rightarrow Mo_2O_4(OH)(H_2O)_6^{3+} + H_2O$	0.17

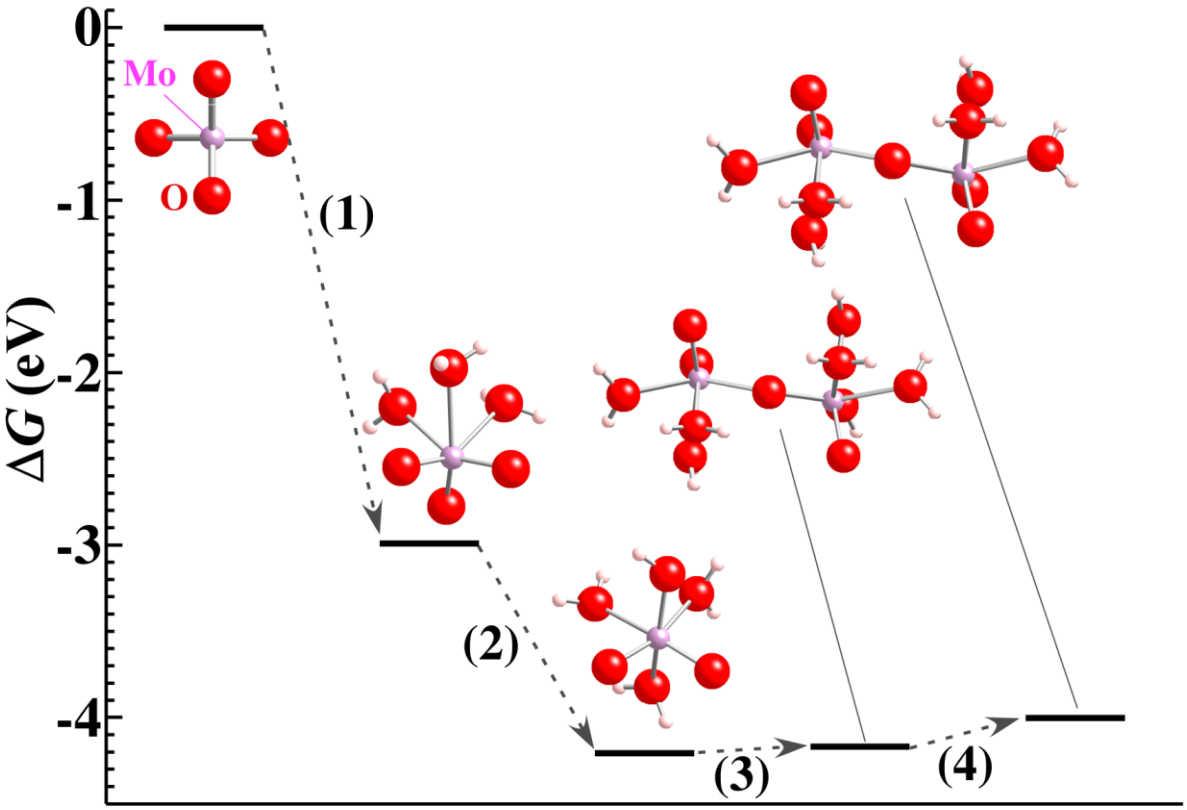

Figure 1. Schematic energy diagram of the free-energy change (ΔG) for the condensation reaction of Mo complexes.

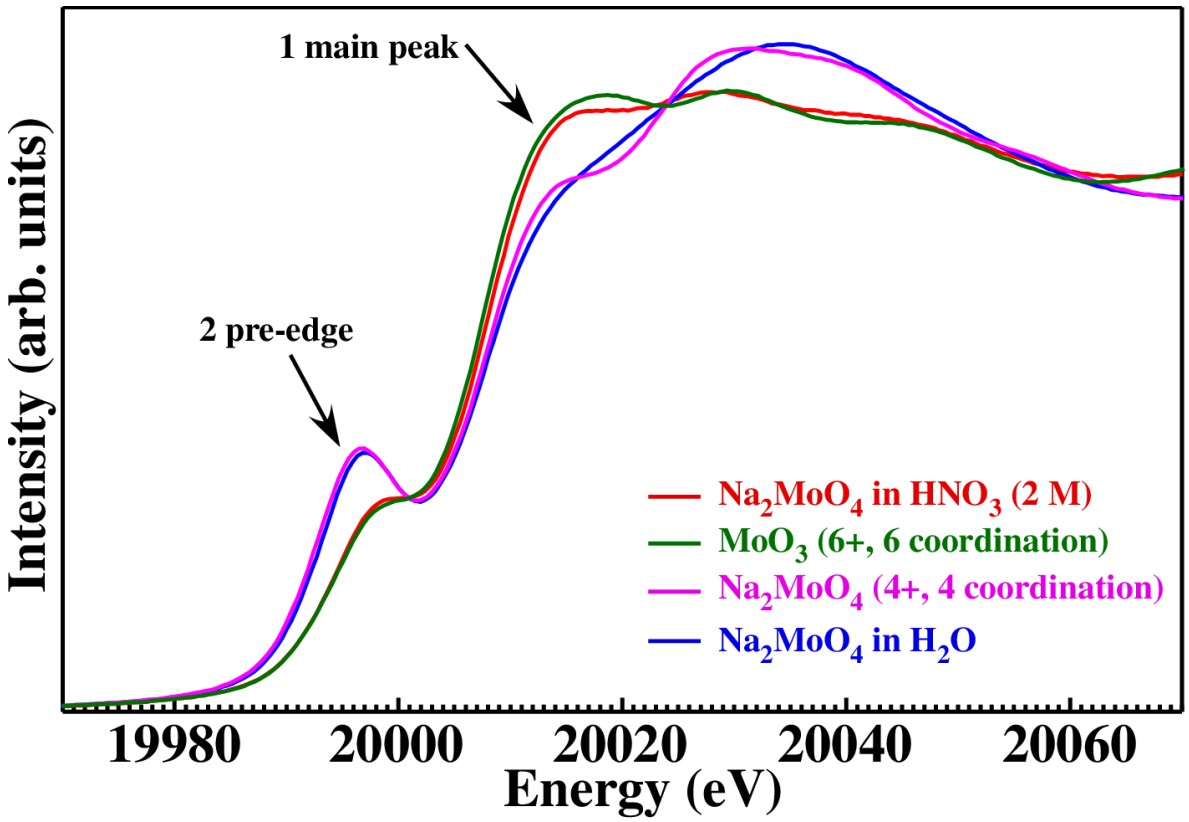

Figure 2. Mo *K*-edge X-ray absorption near edge structure (XANES) spectra of Mo complexes in aqueous (blue) and 2 M nitric acid (red) solution, along with those of $Na_2MoO_4 \cdot 2H_2O$ (pink) and MoO_3 (green) as reference materials.

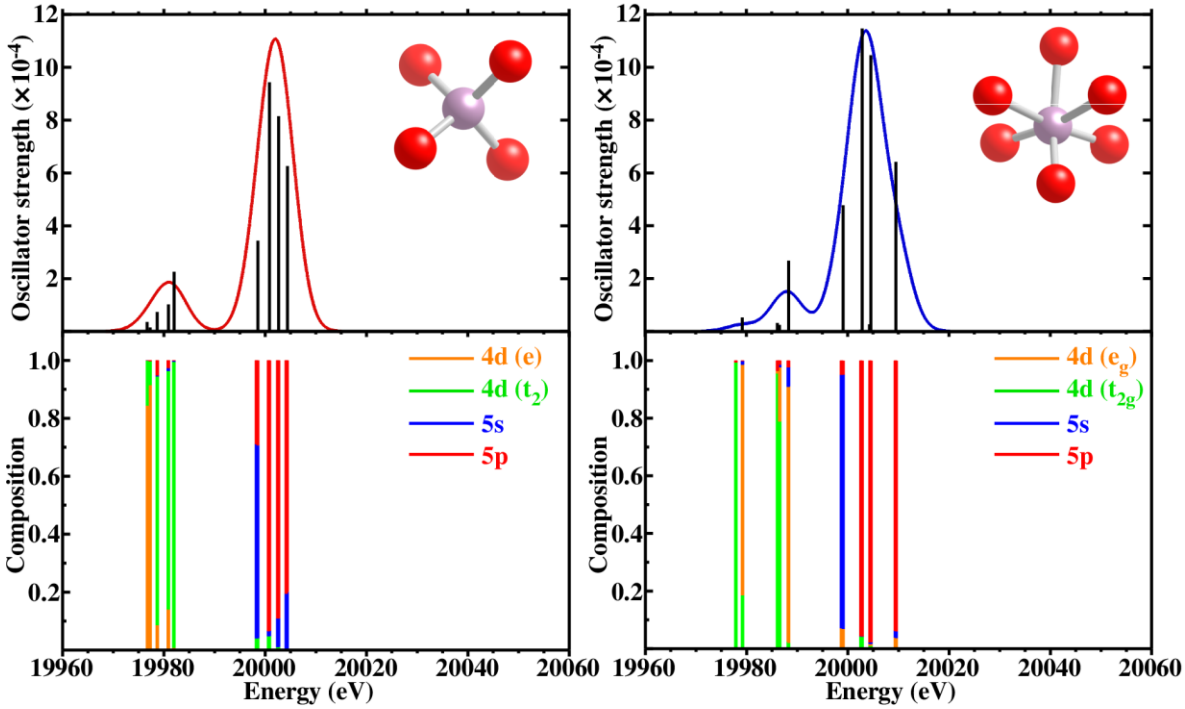

Figure 3. Theoretical Mo K-edge XANES spectra and multiplet energy levels with the corresponding transition components for four- and six-coordinated Mo complexes, which were obtained by first-principles CI calculations. Models of the four- and six-coordinated Mo complexes were constructed from the solid phase of $Na_2MoO_4 \cdot 2H_2O$ and MoO_3, respectively.

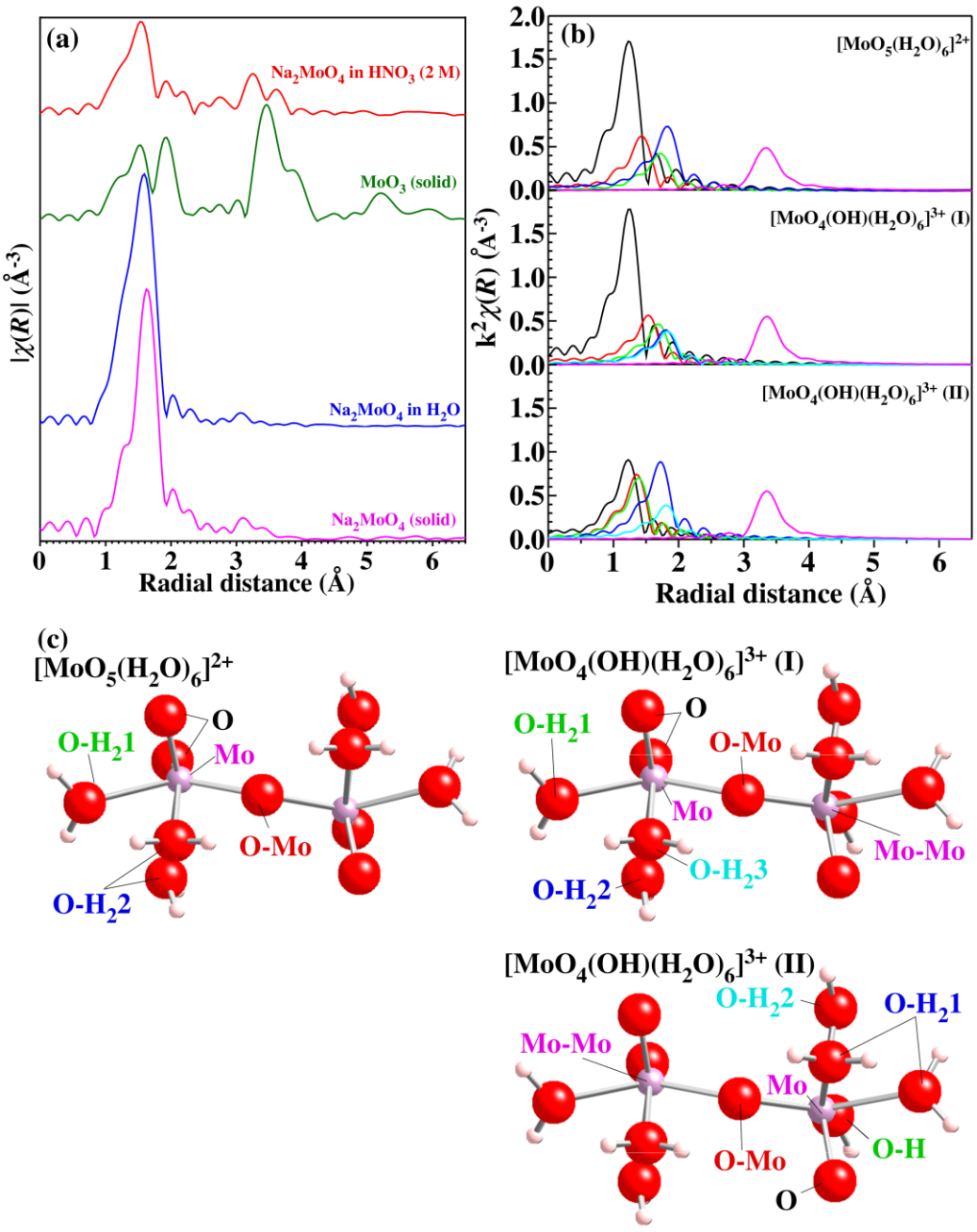

Figure 4. (a) Radial distribution function of XAFS, obtained by extraction with EXAFS, for Mo complex in aqueous solution, 2 M nitric acid solution, $Na_2MoO_4 \cdot 2H_2O$ and MoO_3, (b) the calculated radial distribution function for $[Mo_2O_5(H_2O)_6]^{2+}$ and $[Mo_2O_4(OH)(H_2O)_6]^{3+}$ complex models, using FEFF, where each line represents the oxygen and molybdenum components shown by the same corresponding color, and (c) schematic illustration of each model structure.

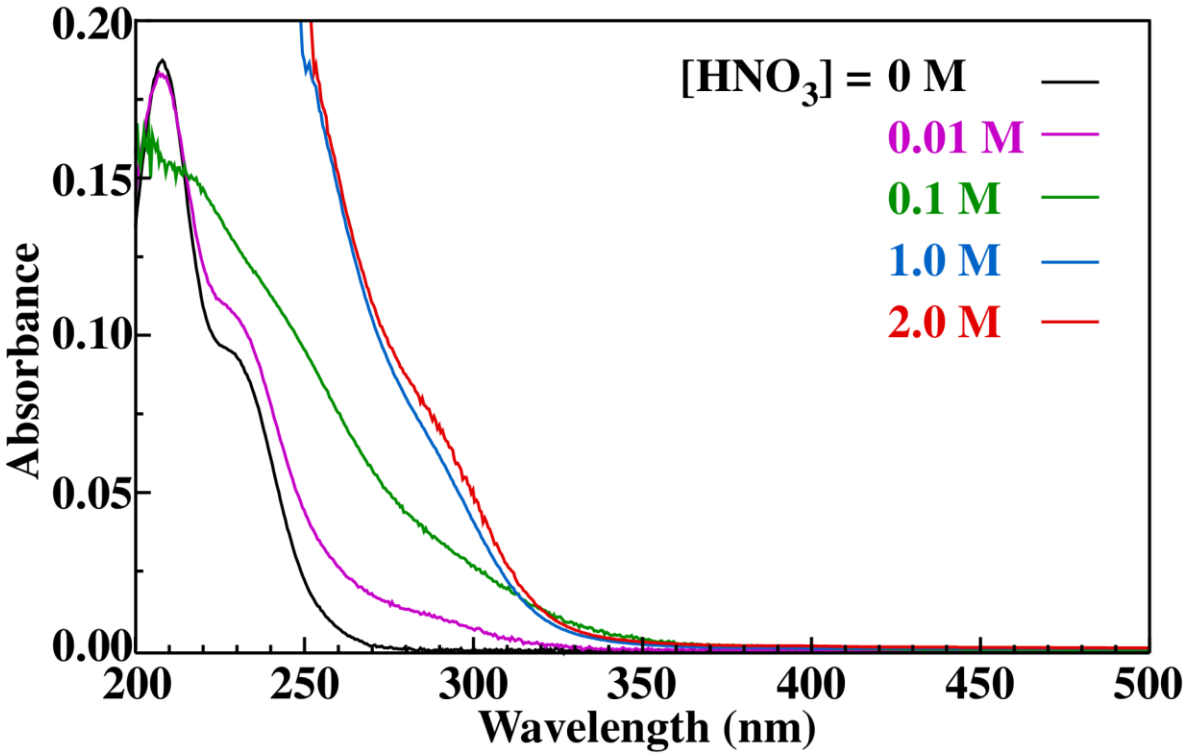

Figure 5. Evolution of experimental UV-Vis absorption spectra with respect to nitric acid concentration for Mo complex.

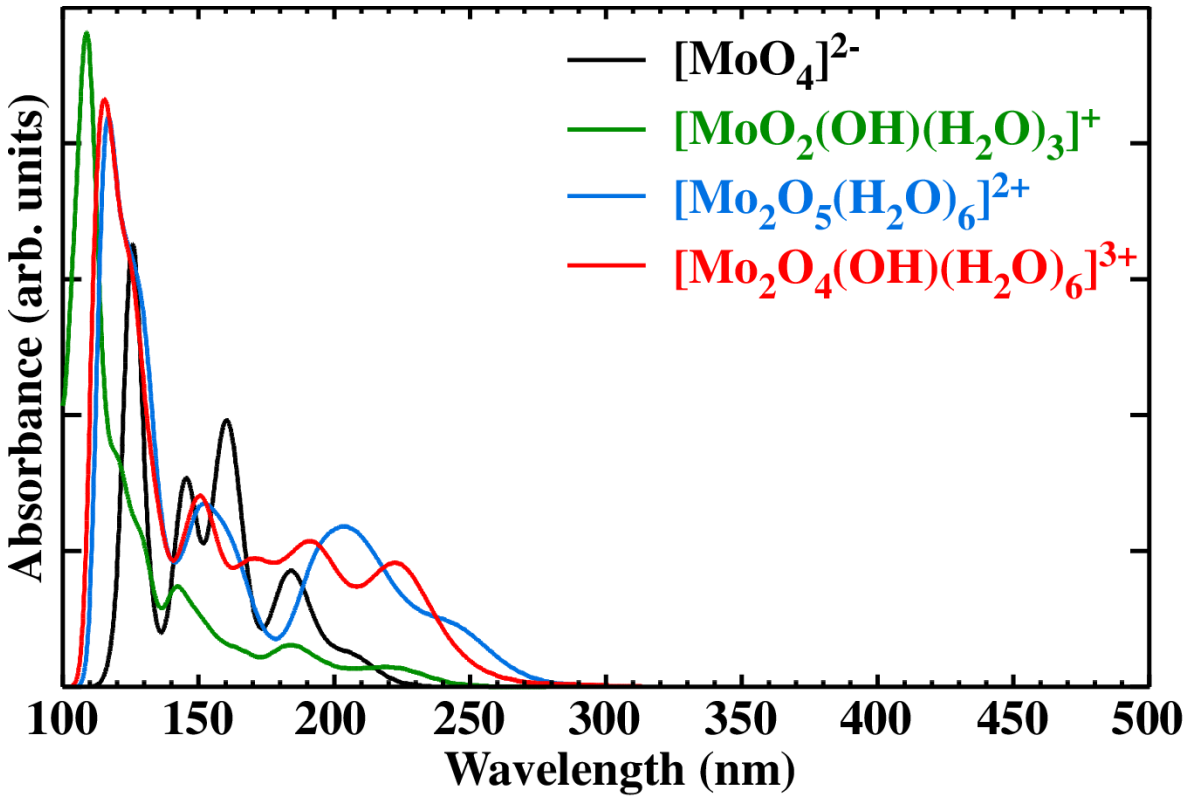

Figure 6. Theoretical UV-Vis absorption spectra of $[MoO_4]^{2-}$, $[MoO_2(OH)(H_2O)_3]^{+}$, $[Mo_2O_5(H_2O)_6]^{2+}$, $[Mo_2O_4(OH)(H_2O)_6]^{3+}$ models by using TDDFT method.